ACS OMEGA

http://pubs.acs.org/journal/acsodf

Article

Projection Diagram for Determining Polarization Curves under Variation of Activation Criterion Using Similarity Theory

Fan Bai and Wen-Quan Tao*

Cite This: *ACS Omega* 2022, 7, 45556−45561

Read Online

ACCESS | Metrics & More | Article Recommendations | Supporting Information

ABSTRACT: Revealing the correlation between polarization curve and input parameters is a highly concerned topic in proton exchange membrane fuel cell (PEMFC) research. Till now, three-dimensional (3D) numerical models have been the most comprehensive methods to predict the polarization curve under variational conditions. However, due to the diversity and complexity of the parameters involved, an immense numerical or experimental burden is required to obtain the above-referred correlation based on 3D numerical model. Application of the similarity theory is considered as a promising breakthrough in PEMFC research to obtain generalized and compact laws. Activation criterion, a relative magnitude of the effect of temperature on electrochemical reaction rate versus the effect of activation overpotential, is the most important criterion on the PEMFC performance. Revealing its impact on the dimensionless polarization curve in the aspects of slope, intercept, and curvature is one of the major challenges for further investigation. Herein, a projection diagram is proposed to determine polarization curves under variation of activation criterion using similarity theory based on a series of results with other criteria variation. As a validation of the concept, two scenarios are exhibited by numerical approach. Results suggest that the maximum relative deviation of polarization curves predicted by the projection diagram is 0.14%, which reaches a high accuracy. The projection diagram reveals the reason why the activation criterion has a comprehensive and complex impact on the dimensionless polarization curve.

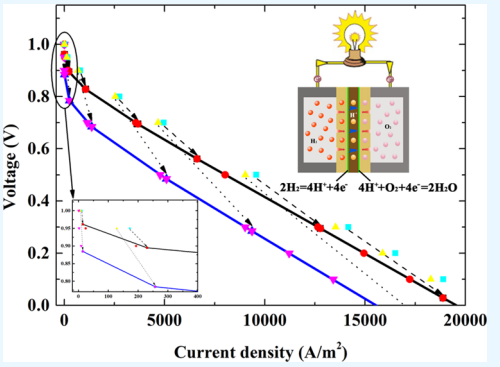

1. INTRODUCTION

Over the past decade, with the coming of the hydrogen era, the commercialization process of a hydrogen energy utilization device, proton exchange membrane fuel cell (PEMFC), has been ever-accelerating.[1−4] The major performance index of the PEMFC is its polarization curve, the relationship between its current versus its output voltage. Predicting the polarization curve under variational conditions is a highly concerned PEMFC research topic. Researchers proposed lots of mathematical−physical models. One of the most classical methods is the semi-empirical model.[5,6] In this model, the correlations of the activation, ohmic and concentration losses as functions of lots of input parameters (for instance, temperature, pressure, diffusivities, transfer coefficients, etc.) are modeled first, and then the polarization curve can be predicted by subtracting all the losses from the reversible voltage. Therefore, the general correlation between the polarization curve and lots of input parameters can be obtained. However, the semi-empirical model is a kind of zero-dimension model. The three-dimensional (3D) distribution of the physical quantities can not be revealed, leading to more possible predicted deviations. At the present stage, polarization curves are commonly theoretically investigated based on a series of complex 3D nonlinear partial differential equations.[7−15] However, the complexity of the nonlinear problem and numerous parameters involved in the models restrict its engineering application.[16] Due to the process complexity of PEMFC, researchers gradually abandon the above-referred general correlation investigation based on a complete 3D PEMFC model. They only reveal the distributions, sensitivity analyses, or other regular patterns under their respective benchmark parameters. Therefore, their detailed research conclusion is very difficult to be expanded to other PEMFC systems.

Similarity theory is an effective tool to obtain generalized and compact results. With its successes in the fields of thermo-fluid science and engineering,[17] electromagnetics,[18] mechanics,[18] ion transport,[19] etc., similarity theory is a promising approach to resolve this issue without reduction of the reliability and accuracy of the mathematical model for the PEMFC.[20] At the present stage, the applications of similarity theory in PEMFC researches have been extensively investigated for the processes in several components of PEMFC, including the flow channel and gas diffusion layer transport

Received: September 28, 2022
Accepted: November 10, 2022
Published: November 30, 2022

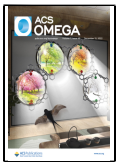

process analysis, membrane electrode assembly (MEA) characteristic and performance analysis, PEMFC contamination measurement research, electrochemical kinetics analysis, etc.[16] For example, in 2005, Gyenge[21] performed dimensional analyses for the Bernardi−Verbrugge one-dimensional numerical model[22] for MEA analysis. The criterion related to the membrane potential difference was expressed as a nonlinear relationship with the criterion related to the current density and two integrated coefficients. In 2007, Chanda and Wang[23] derived four criteria controlling membrane ionic losses. Highly consistent results were obtained after reducing the test data using the four criteria. In 2012, Protsenko and Danilov[24] performed dimensional analysis for the Marcus−Hush−Chidsey formalism for electrochemical kinetics analysis. And based on the derived criteria, the correlation between the reductive reaction rate constant and seven dimensional parameters is constructed. Iranzo et al.[25] recognized the need for using similarity theory for a less expensive description in PEMFC AC impedance analysis. In 2017 and 2019, Russo et al.[26] and Polverino et al.[27,28] also performed similarity theory in AC impedance analysis for reducing the computational and experimental burden.

The above researches make their own great contributions in the performance analyses for different parts of PEMFC using similarity theory. However, due to the complex coupled characteristics, there are few similarity analysis studies focusing on the general correlation between the polarization curve and input parameters, which has more direct significance to PEMFC commercialization. Bai et al.[29] derived seven kinds of input criteria and proposed a dimensionless polarization curve based on a basic multi-physics coupled mathematical model, the three-dimensional single-phase isothermal model, using similarity analysis. Among the input criteria, four criteria relative to the activation loss (eq 1), ohmic loss (eq 2), diffusion mass transfer loss (eq 3), and convection mass transfer loss (eq 4) are of significance to the dimensionless polarization curve, and the dimensionless voltage and dimensionless current density output criteria are shown in eqs 6 and 7, respectively.

$$\mathrm{Act} = \frac{RT}{\alpha n F \eta_t} \tag{1}$$

$$\mathrm{Ohm} = \frac{H_{O_2} A_s J_{0,C} \rho_{O_2} L_t^2}{M_O c_{c,ref}^m \sigma \eta_t} \tag{2}$$

where η_t (V) is the total overpotential calculated by subtracting output cell voltage from the open circuit voltage V_{oc}. For more details about the physical significance of other parameters in this paper, readers may refer to the Supporting Information (Table S1).

$$\mathrm{Dam} = \frac{H_{O_2}}{n, F} \frac{k_{s,j} A_s J_{0,c} L_t^2}{c_{c,ref}^m D}, \; j = O_2, \text{ vapor}, \; k_{s,O_2} = 1, \; k_{s,\text{vapor}} = 1 + 2\beta \tag{3}$$

$$\mathrm{Pe} = \frac{D}{L_t u_{in}} \tag{4}$$

where u_{in} is the inlet velocity calculated by

$$u_{i,in} = \mathrm{St}_i \left(\frac{J_{cell}}{n_i F}\right)\left(\frac{RT}{p_{i,in}}\right)\left(\frac{1}{\omega_{i,in}}\right)\left(\frac{A_{membrane}}{A_{channel,in}}\right) \tag{5}$$

$$\overline{V} = \frac{V_{oc}}{\eta_t} - 1 \tag{6}$$

$$\overline{J} = \frac{J}{H_{O_2} A_S j_{0,C} \rho_{O_{2,in,c}} L_t / M_{O_2} c_{c,ref}^m} \tag{7}$$

The physical meanings of the Act, Ohm, Dam, and Pe are, respectively, a relative magnitude of the effect of temperature on electrochemical reaction rate versus the effect of activation overpotential, a ratio between reference electrochemical reaction rate and conductivity rate, a relative magnitude of the reference electrochemical reaction rate versus diffusion mass transfer, and a ratio between diffusion mass transfer and convection mass transfer. Sensitivity analyses of the above four criteria on the dimensionless polarization curve reveal that the impacts of the three criteria, Ohm, Dam, and Pe, on the dimensionless polarization curve, are mild and to shift the curve. However, the impact of the activation criterion is very significant and complex, which affects the curvature, slope, and intercept with the abscissa of the dimensionless polarization curve.

Above all, revealing the effect of the activation criterion on the polarization curve in detail is one of the major challenges for further general correlation investigation between the output and input criteria in PEMFCs. In this study, a projection diagram is proposed to predict the polarization curve under variation of activation criterion based on the criteria in eqs 1−4, 6, and 7,[29] partially resolving the above-referred general correlation investigation issue. The rest of this paper is organized as follows. In Section 2, the methodology of the projection diagram is introduced. In Section 3, two implementation examples of the proposed projection diagram are presented, and the method is validated. In Section 4, the major observations are concluded.

2. METHODS

In this section, the basic principle and complete procedure of the proposed projection diagram are presented for predicting the polarization curve under variation of activation criterion.

First, the criterion relative to convection mass transfer (Pe, eq 4) is redefined as Mt for the convenience of the subsequent analysis, as follows

$$\mathrm{Mt} = \mathrm{Pe}\cdot\mathrm{Dam}\cdot\overline{J} = \frac{k_{s,j}\omega_{in}}{\mathrm{St}} \frac{A_{channel,in}}{A_{membrane}} \tag{8}$$

The similarity criteria shown in eqs 1−3 and 8 are derived from the closed partial differential equations and boundary conditions governing PEMFC multi-physics process.[29] The voltage boundary condition is standardized as one while the normalization voltage is relative to the output voltage.[29] The dimensionless current density represents the output characteristic of the PEMFC system. Therefore, the correlation between the output and input criteria of PEMFC can be expressed as eq 9

$$\overline{J} = f(\mathrm{Act}, \mathrm{Ohm}, \mathrm{Dam}, \mathrm{Mt}) \tag{9}$$

If the whole polarization curve is considered as the output characteristic, due to the variability of Act and Ohm on the

https://doi.org/10.1021/acsomega.2c06277
ACS Omega 2022, 7, 45556−45561

polarization curve, the correlation can be understood as the function in eq 10

$$\overline{J}\langle\overline{V}\rangle = f(\mathrm{Act}_{\mathrm{ref}}, \mathrm{Ohm}_{\mathrm{ref}}, \mathrm{Dam}, \mathrm{Mt}) \tag{10}$$

where $\overline{J}\langle\overline{V}\rangle$ represents the dimensionless polarization curve and the subscript "ref" represents the corresponding criterion under a reference dimensionless voltage. It should be noted that Dam and Mt are identical on one dimensionless polarization curve, as shown in eqs 3 and 8. Thus, the reference dimensionless voltage is not necessary to be introduced for Dam and Mt in eq 10.

In view of the fact that the output characteristic of PEMFC is generally represented by the whole polarization curve, eq 10 is adopted as PEMFC correlation instead of eq 9. According to eq 9, as long as all the input criteria in two PEMFC systems are identical, the dimensionless current density will also be identical, although the two systems are located in different positions (voltages) on different dimensionless polarization curves represented by eq 10. Therefore, the dimensionless polarization curves under variation of $\mathrm{Act}_{\mathrm{ref}}$ may be projected from the dimensionless polarization curves under a series of groups of other criteria ($\mathrm{Ohm}_{\mathrm{ref}}$, Dam, and Mt). Furthermore, it should be noted that similarity theory itself can only reveal the existence of correlation functions f in eq 9 and 10 instead of the concrete formulations.

According to the above discussions, the general algorithm for the projection diagram can be summarized as follows.

(a) Obtain conventional polarization curves under a series of predesigned groups of $\mathrm{Ohm}_{\mathrm{ref}}$, Dam, and Mt by experimental or numerical approach.
(b) Transform the conventional polarization curves to the dimensionless polarization curves according to eqs 6 and 7.
(c) Obtain the dimensionless polarization curves under variation of activation criterion by a projection diagram from the dimensionless polarization curves in step (b).
(d) Transform the dimensionless polarization curves obtained in step (c) back to the conventional polarization curves for practical application according to eqs 6 and 7.

The predesigned groups in step (a) can be designed under several benchmark criteria ($\mathrm{Act}_{\mathrm{ref},0}$, Dam_0, and Mt_0) and a series of $\mathrm{Ohm}_{\mathrm{ref}}$ criteria, as shown in Figure 1. The dimensionless polarization curves are simplified as straight lines for intuitiveness. The justification of the above design method for step (a) and the corresponding detailed projection method in step (c) will be discussed in this section. The dimensionless polarization curve with $\mathrm{Ohm}_{\mathrm{ref},0}$ is called the original dimensionless polarization curve.

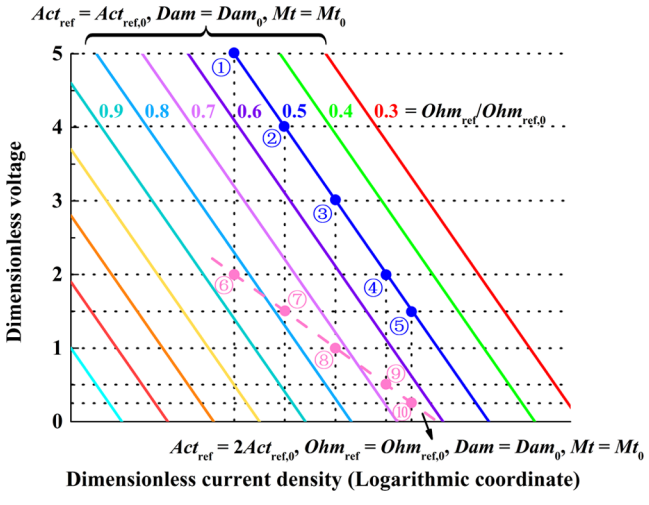

Figure 1. Projection diagram diagrammatic sketch.

Consider the dimensionless polarization curve on which $\mathrm{Ohm}_{\mathrm{ref}}$ is k times compared with $\mathrm{Ohm}_{\mathrm{ref},0}$ (taking $\mathrm{Ohm}_{\mathrm{ref}}/\mathrm{Ohm}_{\mathrm{ref},0} = k = 0.5$ as an example in Figure 1). According to the definition of Ohm, $\mathrm{Ohm}_{\mathrm{ref}}$ conversion relationship between condition 1 and condition 0, which is on the original dimensionless polarization curve with the same dimensionless voltage as condition 1, is shown in eq 11

$$k\mathrm{Ohm}_0 = \mathrm{Ohm}_1 \tag{11}$$

Construct condition 6 in which the overpotential η_t meets eq 12 while other unmentioned criteria are identical to those in condition 0.

$$k\eta_{t,6} = \eta_{t,0} = \eta_{t,1} \tag{12}$$

Substitute eq 12 into eq 11, yielding

$$\mathrm{Ohm}_1 = k\left(\frac{H_{O_2}A_s J_{0,c}\rho_{O_2}L_t^2}{M_{O_2}c_{c,\mathrm{ref}}^m\sigma\eta_{t,0}}\right) = \frac{H_{O_2}A_s J_{0,c}\rho_{O_2}L_t^2}{M_{O_2}c_{c,\mathrm{ref}}^m\sigma\eta_{t,6}} = \mathrm{Ohm}_6 \tag{13}$$

According to the definition of dimensionless voltage, substitute eq 6 into eq 12, yielding

$$\frac{\overline{V}_1 + 1}{\overline{V}_6 + 1} = \frac{1}{k} \tag{14}$$

Among the four input criteria, only Act and Ohm are related to the overpotential η_t. Therefore, the transformation of eq 12 will not affect the values of other criteria. According to eq 12 and the definition of Act shown in eq 1, to guarantee the equivalence of Act in conditions 1 and 6, eq 15 is necessary.

$$k\left(\frac{RT}{\alpha nF}\right)_6 = \left(\frac{RT}{\alpha nF}\right)_1 = \left(\frac{RT}{\alpha nF}\right)_0 \tag{15}$$

It is interesting to note that except electron number of electrochemical reaction n and Faraday constant F, other parameters in eq 15 only appear in the activation criterion. Therefore, Act, Ohm, Dam, and Mt are all identical in conditions 1 and 6. According to eq 9, the dimensionless current densities of the two conditions will also be identical. Condition 6 can be projected from condition 1 perpendicularly to the abscissa based on the dimensionless voltage transformation in eq 14.

Similarly, other corresponding conditions can also be projected based on eq 14, for instance, from 2 to 7, 3 to 8, 4 to 9, and 5 to 10, as shown in Figure 1. A new dimensionless polarization curve is formed by connecting conditions 6, 7, 8, 9, and 10. Furthermore, substitute eq 15 into eq 1, yielding

$$\frac{\mathrm{Act}_{\mathrm{ref,projection}}}{\mathrm{Act}_{\mathrm{ref},\mathrm{Ohm}_{\mathrm{ref}}/\mathrm{Ohm}_{\mathrm{ref},0}=k}} = \frac{1}{k} \tag{16}$$

Therefore, on the projection of dimensionless polarization curve, $\mathrm{Act}_{\mathrm{ref}}$ is $1/k$ times while other criteria are identical compared with the original dimensionless polarization curve.

https://doi.org/10.1021/acsomega.2c06277
ACS Omega 2022, 7, 45556−45561

3. RESULTS AND DISCUSSION

3.1. Validation of Concept. In the current stage, it is hardly possible to validate the proposed projection diagram by the experimental approach due to the difficulty of changing each physical quantity freely. Numerical simulation with proper validation is also an effective approach in PEMFC investigation. In this section, numerical simulations for two scenarios are conducted to validate the correctness of the projection diagram. Readers may refer to our previous study[29] for more details about the governing equations, source terms, boundary conditions, parameters, and validation of the numerical model. In the two scenarios, the activation criteria of the projection polarization curves take 2.0 and 4/3 times compared with the original dimensionless polarization curve, respectively. The physical quantity variations are shown in Table 1. Other benchmark parameters are shown in Table S2[29]

Table 1. Parameters in the Benchmark Scenario (Scenario 0) and the Validation Scenarios (Scenarios 1 and 2) for the Projection Diagram

parameter	scenario 0	scenario 1	scenario 2
α_a	1.0	0.5	0.75
α_c	0.5	0.25	0.375
Act_{ref}	**$Act_{ref,0}$**	**$2Act_{ref,0}$**	**$\frac{4}{3}Act_{ref,0}$**

in the Supporting Information. The numerical results using the parameters in Table 1 are considered as the exact solution for verification, and the dimensionless polarization curve can be obtained according to eqs 6 and 7, as shown by the "▼" and "●" scatter data in Figures 2 and 3.

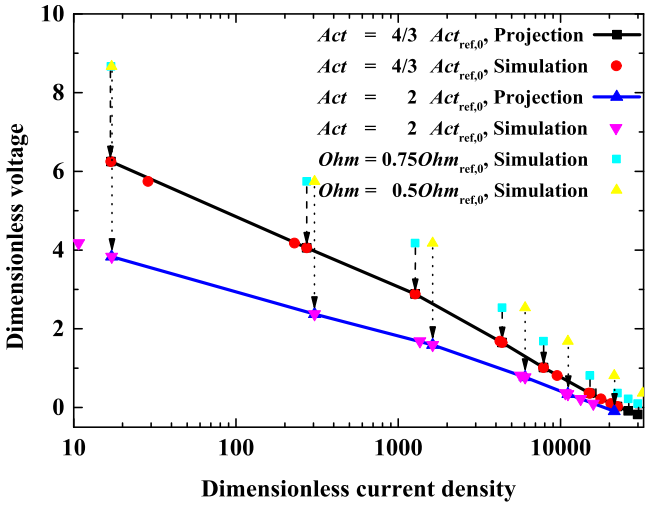

Figure 2. Projection diagram of dimensionless polarization curves.

The dimensionless polarization curves and the dimensional ones under Scenarios 1 and 2 in Table 1 will be obtained by projection diagram in this section. According to Figure 1 and eqs 1−3, 8, and 11, the two scenarios to be projected can be constructed as presented in Table 2. In Table 1 and Table 2, the bold values represent the variable criterion among scenarios in each table. The simulation polarization curves of Scenarios 3 and 4 are exhibited in the scatter data shown by "▲" and "■" in Figure 2. The dimensionless ones can be obtained according to eqs 6 and 7, as shown by the scatter data

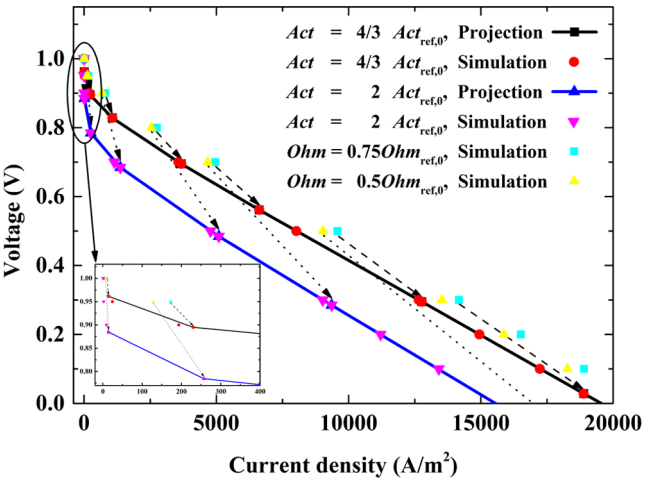

Figure 3. Projection correlation for dimensional polarization curves.

Table 2. Parameters in the Benchmark Scenario (Scenario 0) and the Scenarios to be Projected (Scenarios 3 and 4)

parameter	scenario 0	scenario 3	scenario 4
$A_sJ_{0,a}$	2×10^8	1×10^8	1.5×10^8
$A_sJ_{0,c}$	160	80	120
D_0 (H_2)	9.15×10^{-5}	4.575×10^{-5}	6.8625×10^{-5}
D_0 (O_2)	2.20×10^{-5}	1.1×10^{-5}	1.65×10^{-5}
D_0 (vapor)	2.56×10^{-5}	1.28×10^{-5}	1.92×10^{-5}
Ohm_{ref}	**$Ohm_{ref,0}$**	**0.5 $Ohm_{ref,0}$**	**0.75 $Ohm_{ref,0}$**

of "▲" and "■" in Figure 3. Then, the dimensionless polarization curves of Scenarios 1 and 2 can be projected based on eq 14, as shown by the lines and scatter data "▲" and "■" in Figure 2. Finally, in practice, the dimensional polarization curve is more intuitive to characterize PEMFC performance, which can be obtained according to eqs 6 and 7. The final projected polarization curves (lines and scatter data "▲" and "■") and the dimensional projection correlations are shown in Figure 3. As shown in the figure, we can see that the projection polarization curves are nearly identical to the simulation ones, with a maximum relative deviation of 0.14%, validating the reliability of the projection diagram. Above all, it should be noted that the proposed projection diagram is applicable no matter whether the benchmark parameters shown in Table S2[29] (Supporting Information) take any groups of combinations. Therefore, the general correlation between the polarization curve and activation criterion is modeled based on the proposed projection diagram shown above.

3.2. Discussion. The reason why the activation criterion has a comprehensive and complex impact on the dimensionless polarization curve in the aspects of slope, intercept, and curvature can also be revealed by the projection diagram. The dimensionless polarization curve of Scenario 3 can be expressed by eq 17, which can be obtained by an approximate translation transformation from that of Scenario 0.

$$\overline{V} = g(\overline{J}) \tag{17}$$

Substitute eq 14 into eq 17, yielding the dimensionless polarization curve of Scenario 1, as shown in eq 18

$$\overline{V'} = k(g(\overline{J'}) + 1) - 1 = g'(\overline{J'}) \tag{18}$$

Comparing eqs 17 and 18 for Scenarios 3 and 1, it is obvious that the slope and the intercept of the curve with the abscissa

https://doi.org/10.1021/acsomega.2c06277
ACS Omega 2022, 7, 45556−45561

will vary when the activation criterion changes. Furthermore, from the dimensional polarization curve shown in Figure 3, we can see that with the decrease of current density, the nonlinear characteristic of the polarization curve is more significant, leading to a higher curvature for the dimensionless polarization curve. The dimensionless polarization curve of Scenario 0 can be obtained from an approximate left translation transformation of that in Scenario 3. Therefore, under an identical dimensionless current density, the curvatures of the dimensionless polarization curves in Scenarios 0 and 1 vary. In other words, the activation criterion has impacts on the curvature of the dimensionless polarization curve. Furthermore, although the derived projection diagram is based on PEMFC, the proposed methodology can also be applied in other types of fuel cells based on their corresponding similarity criteria.

4. CONCLUSIONS

This study proposes a projection diagram to obtain the polarization curve under variation of activation criterion. Whereas conventional researches are developed utilizing dimensional physical quantities, which is hardly possible to analyze the general impact of complex and diverse parameters involved in PEMFC models on the polarization curve, the method presented here is based on a more advantageous investigation tool, similarity theory, to obtain generalized and compact results. Validation of the concept is demonstrated for the projection diagram. Results suggest that the maximum relative deviation of polarization curves predicted by the projection diagram is 0.14% compared with the simulation ones, which reaches a high accuracy. Furthermore, it is the projection correlation shown in the diagram that shows the comprehensive and complex impact of the activation criterion on the dimensionless polarization curve in the aspects of both slope, intercept and curvature. Ultimately, the proposed activation diagram plays an important role in the further correlation investigation between output and input parameters in PEMFCs.

■ ASSOCIATED CONTENT

Supporting Information

The Supporting Information is available free of charge at https://pubs.acs.org/doi/10.1021/acsomega.2c06277.

List of symbols and model parameters in this paper (PDF)

■ AUTHOR INFORMATION

Corresponding Author

Wen-Quan Tao − *Shaanxi Collaborative Innovation Center for Hydrogen Fuel Cell Performance Enhancement, Key Laboratory of Thermo-Fluid Science & Engineering of MOE, Xi'an Jiaotong University, Xi'an, Shaanxi 710049, P. R. China;* orcid.org/0000-0002-2348-6299; Email: wqtao@mail.xjtu.edu.cn

Author

Fan Bai − *Shaanxi Collaborative Innovation Center for Hydrogen Fuel Cell Performance Enhancement, Key Laboratory of Thermo-Fluid Science & Engineering of MOE, Xi'an Jiaotong University, Xi'an, Shaanxi 710049, P. R. China*

Complete contact information is available at: https://pubs.acs.org/10.1021/acsomega.2c06277

Author Contributions

The manuscript was written through contributions of all authors. All authors have given approval to the final version of the manuscript.

Notes

The authors declare no competing financial interest.

■ ACKNOWLEDGMENTS

This research was sponsored by the Key Project of National Natural Science Foundation of China (Grant Number 51836005), the Basic Research Project of Shaanxi Province (Grant Number 2019ZDXM3-01), and the Foundation for Innovative Research Groups of the National Natural Science Foundation of China (Grant Number 51721004).

■ REFERENCES

(1) Eudy, L.; Post, M.; Jeffers, M.*American Fuel Cell Bus Project Evaluation: Third Report* (No. NREL/TP-5400-67209). National Renewable Energy Laboratory (US), 2017. https://rosap.ntl.bts.gov/view/dot/36205 (accessed Oct 24, 2022).

(2) Amy, A.Cummins to build railway fuel cell factory. *Railway Gazette International*, November 13, 2020.https://www.railwaygazette.com/business/cummins-to-build-railway-fuel-cell-factory/57781.article?adredir=1 (accessed Oct 24, 2022).

(3) Toshiba Energy Systems & Solutions Corporation Kawasaki Heavy Industries, Ltd. Demonstration Project Begins for Commercialization of Vessels Equipped with High-power Fuel Cells. *Nippon Yusen Kaisha Line*, September 01, 2020. https://www.nyk.com/english/news/2020/20200901_01.html (accessed Oct 24, 2022).

(4) Bai, F.; Quan, H. B.; Yin, R. J.; Zhang, Z.; Jin, S. Q.; He, P.; Mu, Y. T.; Gong, X. M.; Tao, W. Q. Three-dimensional multi-field digital twin technology for proton exchange membrane fuel cells. *Appl. Energy* **2022**, *324*, No. 119763.

(5) Amphlett, J. C.; Baumert, R. M.; Mann, R. F.; Peppley, B. A.; Roberge, P. R.; Harris, T. J. Performance modeling of the Ballard Mark IV solid polymer electrolyte fuel cell: I. Mechanistic model development. *J. Electrochem. Soc.* **1995**, *142*, 1.

(6) Amphlett, J. C.; Baumert, R. M.; Mann, R. F.; Peppley, B. A.; Roberge, P. R.; Harris, T. J. Performance modeling of the Ballard Mark IV solid polymer electrolyte fuel cell: II. Empirical model development. *J. Electrochem. Soc.* **1995**, *142*, 9.

(7) Sivertsen, B. R.; Djilali, N. CFD-based modelling of proton exchange membrane fuel cells. *J. Power Sources* **2005**, *141*, 65−78.

(8) Tao, W. Q.; Min, C. H.; Liu, X. L.; He, Y. L.; Yin, B. H.; Jiang, W. Parameter sensitivity examination and discussion of PEM fuel cell simulation model validation: Part I. Current status of modeling research and model development. *J. Power Sources* **2006**, *160*, 359−373.

(9) Min, C. H.; He, Y. L.; Liu, X. L.; Yin, B. H.; Jiang, W.; Tao, W. Q. Parameter sensitivity examination and discussion of PEM fuel cell simulation model validation: Part II: Results of sensitivity analysis and validation of the model. *J. Power Sources* **2006**, *160*, 374−385.

(10) Kang, S. Quasi-three dimensional dynamic modeling of a proton exchange membrane fuel cell with consideration of two-phase water transport through a gas diffusion layer. *Energy* **2015**, *90*, 1388−1400.

(11) Hu, J.; Li, J.; Xu, L.; Huang, F.; Ouyang, M. Analytical calculation and evaluation of water transport through a proton exchange membrane fuel cell based on a one-dimensional model. *Energy* **2016**, *111*, 869−883.

(12) Jahnke, T.; Futter, G.; Latz, A.; Malkow, T.; Papakonstantinou, G.; Tsotridis, G.; Kompis, C.; et al. Performance and degradation of Proton Exchange Membrane Fuel Cells: State of the art in modeling from atomistic to system scale. *J. Power Sources* **2016**, *304*, 207−233.

(13) Liu, J. X.; Guo, H.; Ye, F.; Ma, C. F. Two-dimensional analytical model of a proton exchange membrane fuel cell. *Energy* **2017**, *119*, 299−308.
(14) Fan, L.; Zhang, G.; Jiao, K. Characteristics of PEMFC operating at high current density with low external humidification. *Energy Convers. Manage.* **2017**, *150*, 763−774.
(15) He, P.; Mu, Y. T.; Park, J. W.; Tao, W. Q. Modeling of the effects of cathode catalyst layer design parameters on performance of polymer electrolyte membrane fuel cell. *Appl. Energy* **2020**, *277*, No. 115555.
(16) Bai, F.; Lei, L.; Zhang, Z.; Chen, L.; Chen, L.; Tao, W. Q. Application of similarity theory in the study of proton exchange membrane fuel cells: A comprehensive review of recent developments and future research requirements. *Energy Storage Sav.* **2022**, *1*, 3−21.
(17) Mikheyev, M.*Fundamentals of Heat Transfer*; Semyonov, S., Ed. (translated from the Russian); Peace Publishers: Moscow, 1956; pp 49−115.
(18) Isaacson, E. de St Q.; Isaacson, M. de St Q.*Dimensional Methods in Engineering and Physics: Reference Sets and the Possibilities of their Extension*; Edward Arnold: London, 1975; 43-59+128−141.
(19) Zhang, J.; Yang, M.; Zhu, H.; Ren, Q.; Qu, Z. Physical similarity and parametric sensitivity analysis of the capacitive deionization process. *Int. J. Green Energy* **2022**, 1−13.
(20) Churchill, S. W. The role of analysis in the rate processes. *Ind. Eng. Chem. Res.* **1992**, *31*, 643−658.
(21) Gyenge, E. L. Dimensionless numbers and correlating equations for the analysis of the membrane-gas diffusion electrode assembly in polymer electrolyte fuel cells. *J. Power Sources* **2005**, *152*, 105−121.
(22) Bernardi, D. M.; Verbrugge, M. W. A mathematical model of the solid-polymer-electrolyte fuel cell. *J. Electrochem. Soc.* **1992**, *139*, 2477.
(23) Chanda, S.; Wang, X. Study of membrane ionic losses in a PEM fuel cell using dimensional analysis. *ECS Trans.* **2007**, *11*, 1165.
(24) Protsenko, V. S.; Danilov, F. I. Application of dimensional analysis and similarity theory for simulation of electrode kinetics described by the Marcus−Hush−Chidsey formalism. *J. Electroanal. Chem.* **2012**, *669*, 50−54.
(25) Iranzo, A.; Muñoz, M.; Pino, F. J.; Rosa, F. Non-dimensional analysis of PEM fuel cell phenomena by means of AC impedance measurements. *J. Power Sources* **2011**, *196*, 4264−4269.
(26) Russo, L.; Sorrentino, M.; Polverino, P.; Pianese, C. Application of buckingham π theorem for scaling-up oriented fast modelling of proton exchange membrane fuel cell impedance. *J. Power Sources* **2017**, *353*, 277−286.
(27) Polverino, P.; Bove, G.; Sorrentino, M.; Pianese, C. Generalized scaling-up approach based on Buckingham theorem for Polymer Electrolyte Membrane Fuel Cells impedance simulation. *Energy Procedia* **2019**, *158*, 1514−1520.
(28) Polverino, P.; Bove, G.; Sorrentino, M.; Pianese, C.; Beretta, D. Advancements on scaling-up simulation of Proton Exchange Membrane Fuel Cells impedance through Buckingham Pi theorem. *Appl. Energy* **2019**, *249*, 245−252.
(29) Bai, F.; Lei, L.; Zhang, Z.; Li, H.; Yan, J.; Chen, L.; Dai, Y.; Chen, L.; Tao, W. Q. Application of similarity theory in modeling the output characteristics of proton exchange membrane fuel cell. *Int. J. Hydrogen Energy* **2021**, *46*, 36940−36953.

https://doi.org/10.1021/acsomega.2c06277
ACS Omega 2022, 7, 45556−45561